

# Design of Azimuthally Periodic Wedge-Shaped Circular Ring Bandpass Frequency Selective Surface Using Transmission-Line Method

Garima Bharti<sup>1</sup> · Kumud Ranjan Jha<sup>2</sup> · G. Singh<sup>1</sup> ·  
Rajeev Jyoti<sup>3</sup>

Published online: 23 June 2015  
© Springer Science+Business Media New York 2015

**Abstract** In this paper, an azimuthally periodic wedge-shaped circular aperture frequency selective surface (FSS) is discussed, which provides the dual polarized and angular stable frequency response with significantly more fractional bandwidth (FBW) up to 50° angle-of-incidence (AOI) at S-band, Ku-band and Ka-band. In addition to this, the equivalent circuit (EC) parameters of proposed bandpass FSS structure are obtained using the transmission-line approach, which are further utilized to compute the geometrical parameters of the proposed bandpass FSS structure at 3, 15 and 25 GHz. The numerical results computed by transmission-line approach are supported with the simulation results, which have been obtained using commercially available simulators such as CST Microwave Studio (finite integral technique) and Ansoft HFSS (finite element method) at each frequency of interest.

**Keywords** Frequency selective surface · Angular/polarization stable · Transmission-line method · Equivalent circuit technique · Fractional bandwidth

---

✉ G. Singh  
ghanshyam.singh@juit.ac.in  
Garima Bharti  
ergarimabharti25@gmail.com  
Kumud Ranjan Jha  
kumud.ranjan@smvdu.ac.in  
Rajeev Jyoti  
rajeevjyoti@sac.isro.gov.in

<sup>1</sup> Department of Electronics and Communication Engineering, Jaypee University of Information Technology, Solan 173 234, India

<sup>2</sup> School of Electronics and Communication Engineering, Shri Mata Vaishno Devi University, Katra, Jammu and Kashmir 182 301, India

<sup>3</sup> Space Application Centre, Indian Space Research Organization, Ahmadabad, India

## 1 Introduction

Frequency selective surface structures have a potential to impart the bandstop and bandpass spatial filtering characteristics, which ideally provides the total reflection and transmission response at the resonance frequency, respectively [1]. These spatial filters in one or the other form provide various applications in space/satellite communication, antenna systems [reducing the radar cross-section (RCS)], electromagnetic shielding, frequency-selective windows and waveguide filters [2–8]. The bandstop FSS structures allow the propagation of direct current signals through it, which is not suitable for various applications as discussed in [1]. Therefore, recently the demand of designing the bandpass FSS structures has been increased, which are very useful for the modification of electromagnetic architecture of buildings to accommodate the advanced and imminent wireless technologies [9–11]. There are various reported numerical techniques to obtain the resonance behaviour of FSS structures such as three-dimensional full-wave finite element method (FEM) [12], finite difference time domain (FDTD) codes [13], method-of-moment (MoM) [14, 15] and EC [16, 17]. Moreover, the numerical techniques discussed in [12–15] provide the extensive computations. Therefore, in order to obtain an immediate knowledge of the electromagnetic properties of FSS structures such as scattering, reflection and transmission, an EC analysis, which is based on the approximation of FSS structure as a lumped circuit parameters, is adopted [16, 17]. In addition to this, the EC approach also provides significant insight into the physical and design properties of the periodic structure as compared to that of the full-wave numerical techniques [18–21].

However, there are various FSS structures, which have been discussed in the existing literatures such as square loop [22–26], circular ring [27, 28], tunable FSSs [29] and different novel FSS structures [30–33]. It has been discussed in [22–28] that the conventional square loop and circular ring FSS offer significant angular stability over a wide range of AOIs and different polarizations due to their symmetrical nature. In [30], the active circular ring, which is loaded with the varactor diode, has been discussed. In [31], the effect of the perpendicular and parallel polarized wave incidence up to 60° AOI has been discussed on the FSS structure, which has four spiral rectangles connected to a cross-line element in the middle. In [32], the angular (up to 60°) and polarization sensitivity of the FSS structure, which has four symmetrical spiral patterns of metallic meander line printed on FR4 dielectric substrate, has been discussed. Yan et al. [33] have discussed the FSS structure, which has four symmetrical spiral patterns of metallic meander line printed on F4B-2 dielectric substrate for perpendicular and parallel wave incident up to 60°. In [34], the frequency response of a thick screen four legged loaded FSS structure has been discussed for perpendicular and parallel polarized wave incidence up to 60° AOI.

It has been discussed that the conventional circular ring FSS provides significant FBW as compared to that of the square loop FSS and outperforms the square loop FSS structure [1]. Recently, we have reported an azimuthally periodic wedge-shaped metal vane loaded circular ring FSS structure for bandstop filtering characteristics in Ku-band [34], which provides significantly better angular stability and FBW as compared to that of the conventional circular ring FSS structure. Therefore, we have extended this work [34] for the bandpass filtering characteristics in S/Ka and Ku-band of the electromagnetic spectrum. The proposed bandpass FSS structure provides significantly better angular/polarization stability as compared to that of the conventional geometrical shapes such as square loop [22–26], circular ring [27], active circular ring (loaded with varactor diode) [29] as well as recently reported novel FSS structures [30–33]. Moreover, the proposed bandpass FSS has

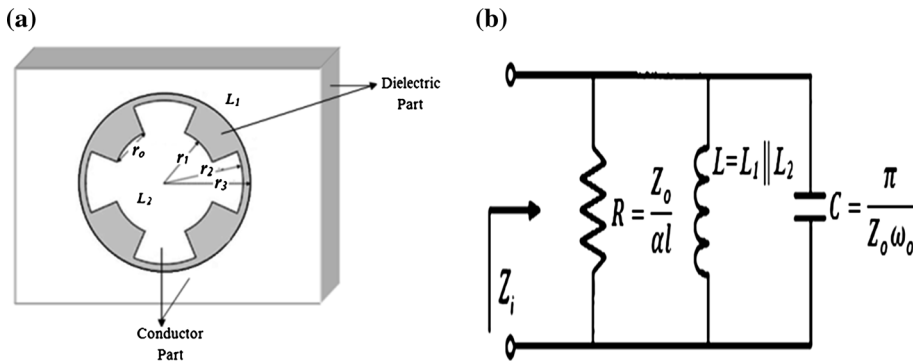


**Fig. 1** The azimuthally periodic wedge-shaped circular ring bandpass FSS (a) unit-cell configuration, and (b) its equivalent circuit

a very thin overall thickness of  $0.007\lambda$  (at 3 GHz), where  $\lambda$  is the smallest wavelength in the operating wavelength range, which prevents the generation of surface waves especially at the large incidence angles and provide significances in the shielding applications.

The resonance behaviour of the proposed bandpass FSS structure is discussed by considering it as the two port network, which has randomly selected input/output port along the circumference of the proposed bandpass structure, and a transmission-line model is used to extract the equivalent lumped circuit elements such as inductance ( $L$ ) and capacitance ( $C$ ). The port analysis of the proposed bandpass FSS structure provides a parallel RLC circuit, which has resistance ( $R$ ), capacitance ( $C$ ) and an equivalent inductance ( $L = L_1 \parallel L_2$ ), where  $L_1$  and  $L_2$  is the inductance due to the conducting portion, which is shown in Fig. 1a. For the lossless FSS structure, the value of  $R$  vanishes. The remainder of the paper is organized as follows. Section 2 discusses the theory of operation, which includes the EC realization and the synthesis of the geometrical parameters of the proposed bandpass FSS structure. Section 3 discusses the resonance behaviour of the proposed FSS structure at 3, 15 and 25 GHz for the perpendicular and parallel polarized waves, which have been incidence up to  $50^\circ$  AOI. Finally, Sect. 4 concludes the work.

## 2 Theory of Operation

### 2.1 Equivalent Circuit Realization

In this paper, we have discussed the resonance behaviour of an azimuthally periodic wedge-shaped circular ring bandpass FSS structure, which is shown in Fig. 1a with its geometrical parameters such as periodicity ( $p$ ), outer radius of the circular aperture ( $r_3$ ), inner radius of the circular aperture ( $r_2$ ), inner radius of wedge-shaped aperture ( $r_1$ ), width of the circular aperture ( $w_1$ ), which results from the  $(r_3 - r_2)$  and width of the wedge shaped aperture ( $w_2$ ), which results from the  $(r_2 - r_1)$ . The periphery of circular aperture must be equal or integer multiple of resonance frequency, which provides the equivalent inductance and width of aperture corresponds to the capacitance of the proposed FSS structure [35, 36]. As discussed in [16], if the width of circular ring is narrow (in the microwave regime), then circular ring resonator exhibits same dispersion characteristics as that of the transmission-line resonator, therefore the ring resonator has been analyzed using the transmission-line model. Similarly,

the electrical equivalent behaviour of the proposed bandpass FSS structure has been analyzed using the two-port network based on the transmission-line model [16].

The proposed bandpass FSS structure has been represented in terms of the parallel RLC circuit using the EC approach as shown in Fig. 1b. However, the input impedance of the proposed bandpass FSS structure in terms of the parallel RLC circuit is given as [37]:

$$Z_i = \frac{R}{1 + 2j\Delta\omega CR} \tag{1}$$

where,  $Z_i$ ,  $R$  and  $C$  are the input impedance, resistance in  $\Omega$  and capacitance of the proposed bandpass FSS structure, respectively. In addition to this, the transmission-line model is used to obtain the input impedance of the proposed bandpass FSS structure. For the transmission-line model, the input impedance in terms of the Y-parameters, which have been achieved through the ABCD matrix, is given as [16]:

$$Z_{ic} = \frac{Z_o\omega_r}{\alpha l\omega_r + 2j\Delta\omega\pi} \tag{2}$$

where,  $Z_{ic}$ ,  $Z_o$ ,  $\alpha$ ,  $l$ ,  $\omega_r$  and  $\Delta\omega$  are the input impedance, characteristic impedance, attenuation constant, length which represents the mean circumference, resonance angular frequency and small deviation in the angular frequency of the transmission-line model, respectively of the transmission-line model. However, with the comparison of Eqs. (1) and (2), we have achieved the resistance and capacitance as follows.

$$R = \frac{Z_o}{\alpha l} \quad \text{and} \quad C = \frac{\pi}{Z_o\omega_r} \tag{3}$$

In the proposed bandpass FSS structure, the equivalent inductance ( $L$ ) is equal to  $L_1 \parallel L_2$ . Here,  $L_1$  is given as [38]:

$$L_1(nH) = 1.257 \times 10^{-3} a \left[ \ln\left(\frac{a}{w_1 + t}\right) + 0.078 \right] \cdot K_g \tag{4}$$

where,  $a$ ,  $w_1$ ,  $t$  and  $K_g$  are the mean radius  $a = ((r_3 + r_2)/2)$ , width of the circular aperture, thickness of the conductor and correction factor, respectively. In general, Eq. (4) is used to find the value of the microstrip inductance above the grounded substrate. However, in the case of FSS structure, the ground plane beneath the substrate is not used. Therefore, the correction factor  $K_g$  which provides the effect of electric field between the microstrip structure and ground plane, which is set equal to the unity as discussed in detail in [38]. In addition to this,  $L_2$  is obtained as:

$$L_2(nH) = 2n \times 10^{-4} r_o \left[ \ln\left(\frac{r_o}{w_2 + t}\right) + 1.193 + \left(\frac{w_2 + t}{3r_o}\right) \right] \cdot K_g \cdot \sin \theta \tag{5}$$

**Table 1** The geometrical parameters of the proposed bandpass FSS structure at 3, 15 and 25 GHz

Operating Frequency (GHz)	$r_1$ (mm)	$r_2$ (mm)	$r_3$ (mm)
3	8.0	12	18
15	2.0	2.4	3.0
			83
25	0.5	1.1	1.9

**Table 2** Angular stability and 3-dB reflection/transmission bandwidth of the proposed bandpass FSS structure through CST Microwave Studio and Ansoft HFSS in S-band for perpendicular and parallel polarized wave

AOI	Perpendicular polarization						Parallel polarization					
	CST MWS			Ansoft HFSS			CST MWS			Ansoft HFSS		
	$f_r$ (GHz)	3-dB BW (GHz)	FBW (%)	$f_r$ (GHz)	3-dB BW (GHz)	FBW (%)	$f_r$ (GHz)	3-dB BW (GHz)	FBW (%)	$f_r$ (GHz)	3-dB BW (GHz)	FBW (%)
0°	3.360	2.5537	76	3.40	2.60	76.47	3.392	2.4988	70.7	3.40	2.40	70.5
10°	3.356	2.4829	73.9	3.40	2.50	73.5	3.383	2.3632	69.8	3.40	2.40	70.5
30°	3.342	2.0228	60.5	3.39	2.10	61.9	3.381	2.2398	66.2	3.38	2.20	65.0
50°	3.334	1.986	59.5	3.38	2.00	59.1	3.370	2.2029	65.3	3.38	2.20	65.0

and

$$L = L_1 \parallel L_2 \tag{6}$$

where  $n$ ,  $r_0$ ,  $w_2$  and  $\theta$  are the number of vanes, length of the arc of vanes, width of the wedge-shaped aperture and AOI, respectively. All the dimensions have been chosen in micrometer ( $\mu\text{m}$ ). Therefore, the resonance frequency of the proposed bandpass FSS structure is given as:  $f_r = \frac{1}{2\pi\sqrt{LC}}$ .

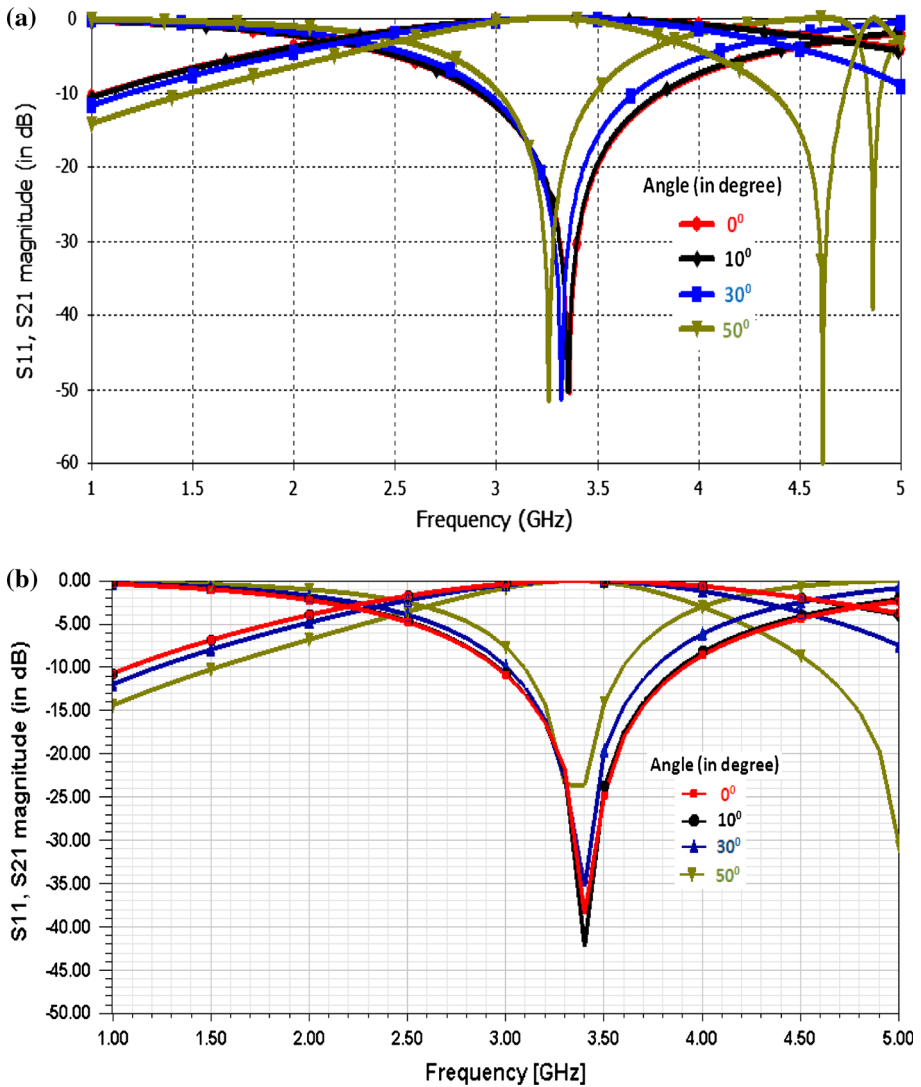


**Fig. 2** The frequency response of proposed bandpass FSS structure for perpendicular polarized wave at different AOI in S-band using (a) CST Microwave Studio and (b) Ansoft HFSS

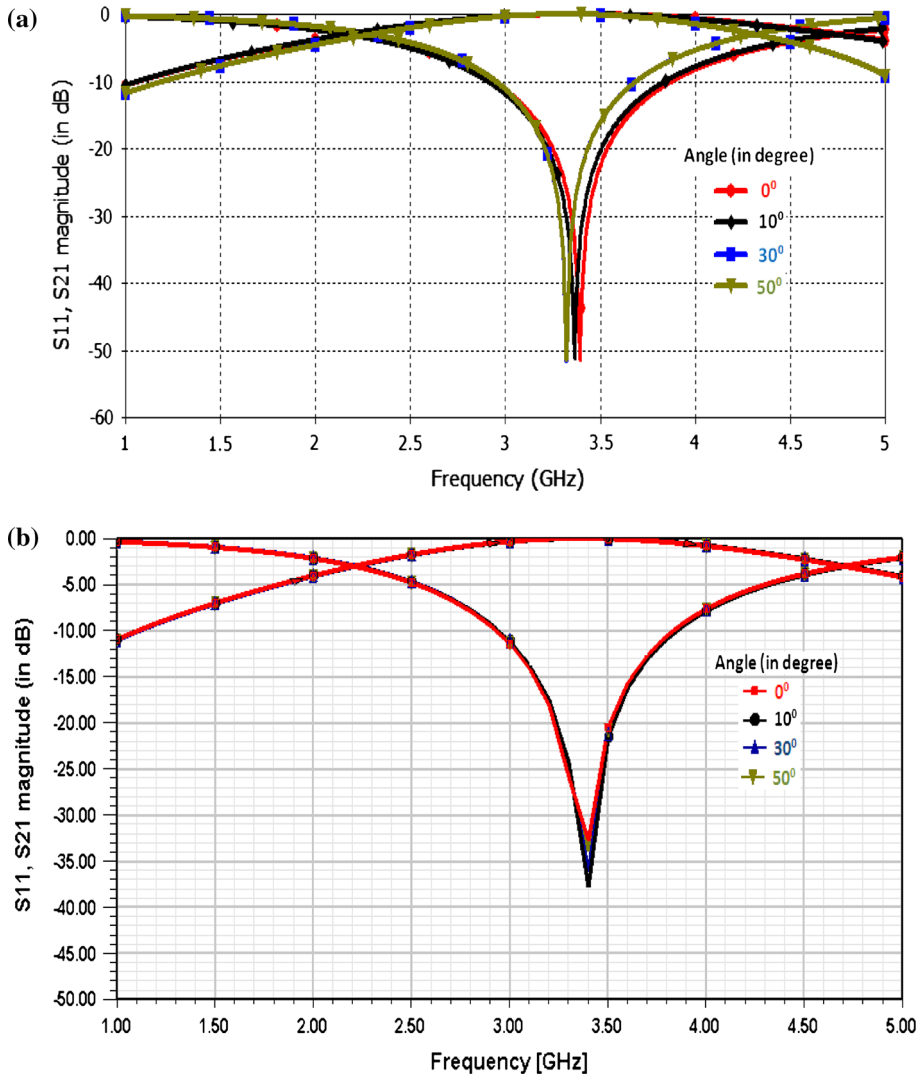


**Fig. 3** The frequency response of proposed bandpass FSS structure for parallel polarized wave at different AOIs using in S-band (a) CST Microwave Studio and (b) Ansoft HFSS

### 2.2 Parametric Synthesis

The mean radius of proposed bandpass FSS structure is given as [1]:  $2\pi r = \lambda_o / \sqrt{\epsilon_{eff}}$ , where,  $r$ ,  $\lambda_o$  and  $\epsilon_{eff}$  are the mean radius, operating wavelength and effective dielectric permittivity, respectively. Further, we have computed the value of  $C$  for each operating frequency using Eq. (3) and value of  $L_1$  using Eq. (4). In addition to this, we have tuned the value of  $L_2$  by varying the associated geometrical parameters in order to achieve the appropriate value of  $L$ , which provides the desired/intended resonance frequency. We have computed the values of  $L$  and  $C$ , which represent the unit-cell of proposed bandpass FSS structure at normal wave incidence for 3, 15 and 25 GHz. Using the theory discussed in

**Table 3** Angular stability and 3-dB reflection/transmission bandwidth of the proposed bandpass FSS structure through CST Microwave Studio and Ansoft HFSS in Ku-band for perpendicular and parallel polarized wave

AOI	Perpendicular polarization		Parallel polarization	
	CST MWS $f_r$ (GHz) 3-dB BW	Ansoft HFSS $f_r$ (GHz) 3-dB BW	CST MWS $f_r$ (GHz) 3-dB BW	Ansoft HFSS $f_r$ (GHz) 3-dB BW
0°	15.144	15.15 2.60	15.174 2.5988	15.20 2.50
10°	15.144	15.15 2.50	15.168 2.56	15.20 2.50
30°	15.142	15.12 2.30	15.156 2.0398	15.20 2.40
50°	15.142	15.03 2.20	15.144 2.0229	15.20 2.40

this Section, the geometrical parameters computed at each frequency of interest such as at 3, 15 and 25 GHz are shown in Table 1.

### 3 Design and Simulation

In this section, the proposed bandpass FSS structure is designed at 3, 15 and 25 GHz using the commercial simulators such as CST Microwave Studio and Ansoft HFSS. To design the unit-cell of proposed bandpass FSS structure, Arlon AD 320 is used as dielectric substrate (dielectric permittivity,  $\epsilon_r = 3.2$ ,  $\tan\delta = 0.0028$  and thickness 0.762 mm) and copper is used as a conductive sheet (electrical conductivity,  $\sigma = 5.8 \times 10^7$  S/m and thickness,  $t = 0.02$  mm). In this section, the angular stability, 3-dB reflection/transmission bandwidth and FBW of the proposed bandpass FSS structure for perpendicular and parallel polarized wave, which has been incidence up to 50° AOI at 3, 15 and 25 GHz, are presented. In addition to this, we have also explored the electric field distribution of the proposed bandpass FSS at each frequency of interest for the normal wave-incidence.

#### 3.1 Angular/Polarization stability

The values of  $r_1$ ,  $r_2$  and  $r_3$  at  $f_r = 3$  GHz are as demonstrated in the first row of Table 1. In addition to this, the characteristic impedance,  $Z_0 = 377 \Omega$ , mean radius,  $a = 15$  mm,  $w_1 = 6$  mm,  $w_2 = 4$  mm and  $r_o = 6.280$  mm. The value of capacitance  $C$  is computed using Eq. (3) that is 0.442 pF. Further, the value of inductance  $L_1$  [using Eq. (4)] and  $L_2$  [using Eq. (5)] are computed as 18.68 and 9.30 nH, respectively. Moreover, the value of  $L$  (nH) is computed using Eq. (6), which is 18.68 nH ||9.30 nH and results the 6.20 nH. The proposed FSS structure resonates at 3.1 GHz for normal wave incidence, which has equivalent circuit parameters such as  $C$  and  $L$  are 0.442 pF and 6.20 nH, respectively. Table 2 discusses the effect of perpendicular and parallel polarized wave incidence up to 50° AOI on the resonance frequency, 3-dB bandwidth and FBW of the proposed bandpass FSS structure. For the perpendicular and parallel polarized wave incidence up to 50° AOI on the proposed bandpass FSS, the FBW of approximately 59 and 65 % have been achieved as illustrated in Table 2, respectively. For the perpendicular polarized wave incidence up to 50° AOI, the resonance frequency of the proposed bandpass FSS structure downshifts up to 0.77 % with reference to the normal wave incidence which is computed by using CST Microwave Studio as shown in Fig. 2a. However, this downshift is order of

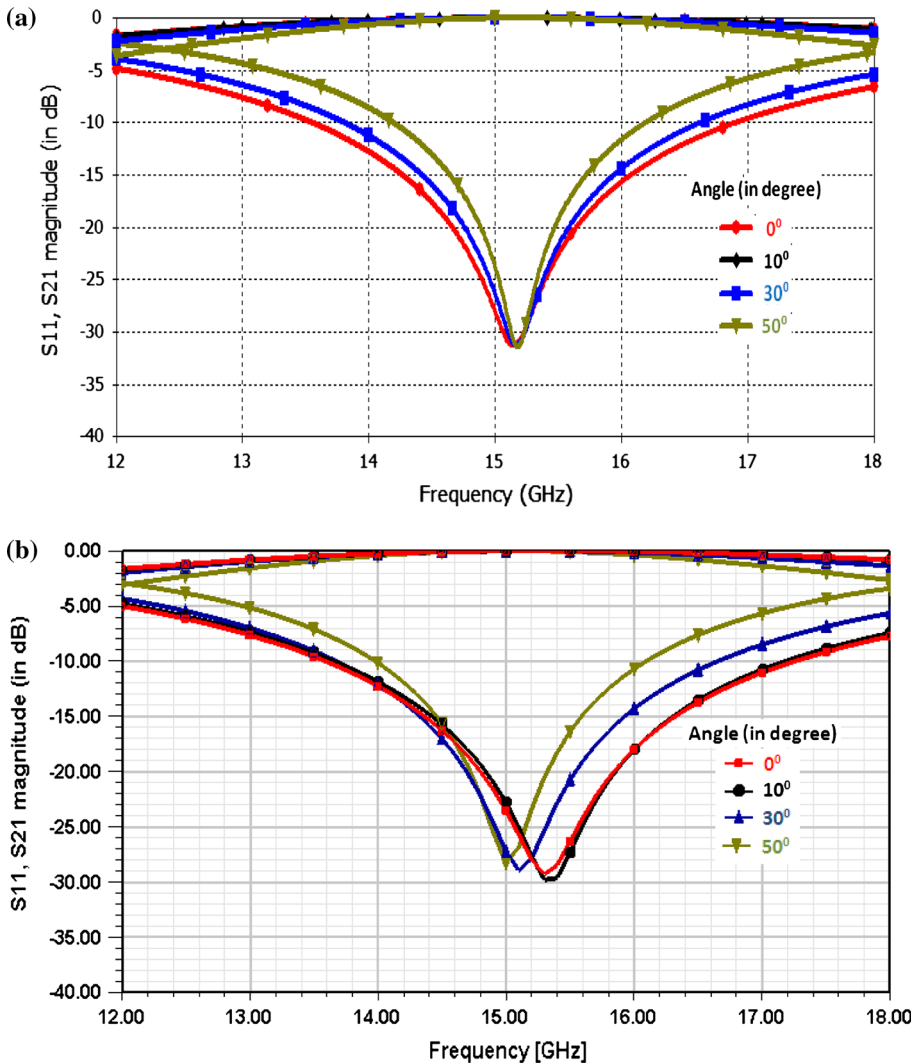


**Fig. 4** The frequency response of proposed bandpass FSS structure for perpendicular polarized wave at different AOI in Ku-band using (a) CST Microwave Studio and (b) Ansoft HFSS

0.56% when the simulation is performed using Ansoft HFSS as shown in Fig. 2b. Figure 3a, b demonstrate 0.65 and 0.59% downshift in the resonance frequency with reference to the normal wave incidence using CST Microwave Studio and Ansoft HFSS, respectively, for the parallel polarized wave incidence up to 50°.

On the similar way, the Eqs. (3) and (6) have been used to compute the value of  $C$  and  $L$  at 15 GHz, which are 0.884 fF and 1.29 nH, respectively, and results the resonance frequency of 14.98 GHz at normal wave incidence. Table 3 illustrates the effect of the perpendicular and parallel polarized wave incidence up to 50° AOI on the resonance frequency and 3-dB bandwidth of the proposed bandpass FSS structure. Figure 4a, b demonstrate 0.013 and 0.79% downshift in the resonance frequency with reference to the

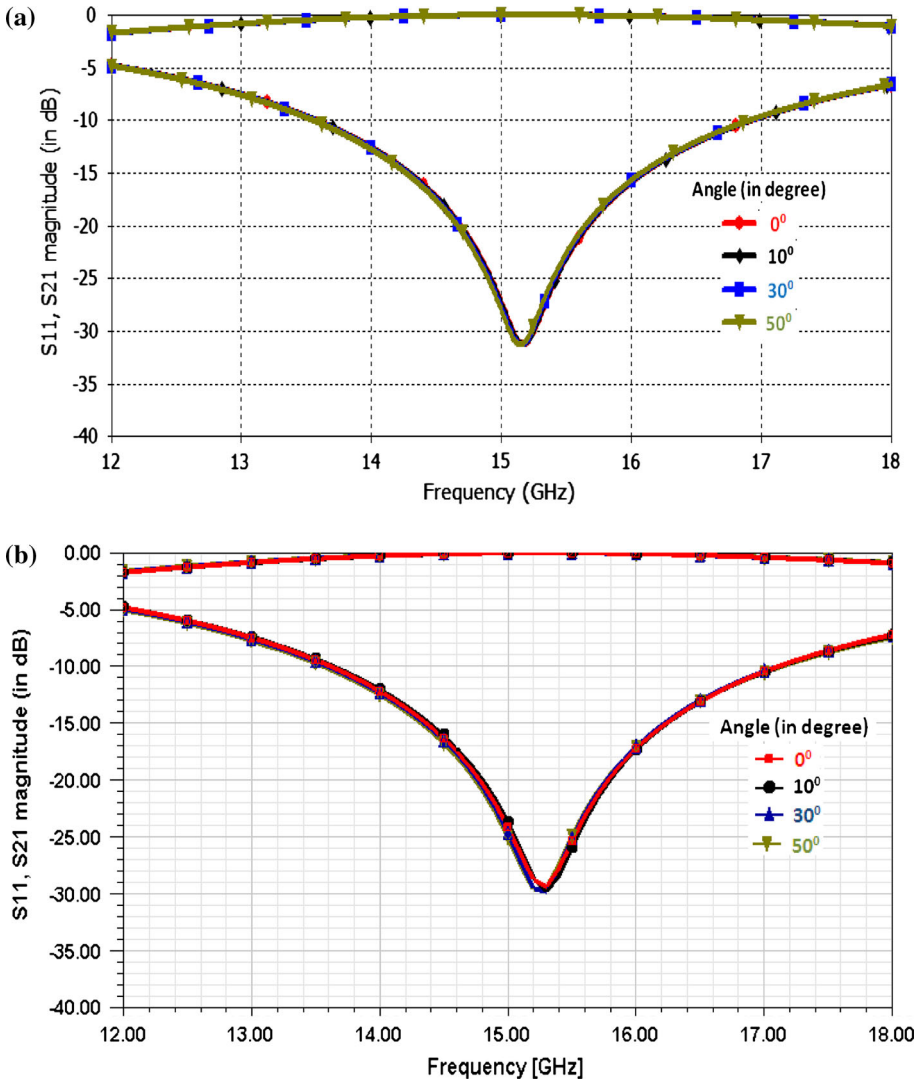


**Fig. 5** The frequency response of proposed bandpass FSS structure for parallel polarized wave at different AOI in Ku-band using (a) CST Microwave Studio and (b) Ansoft HFSS

normal incidence using CST Microwave Studio and Ansoft HFSS, for perpendicular polarized wave up to 50° AOI, respectively. Figure 5a demonstrates 0.198 % downshift in the resonance frequency with reference to the normal wave incidence for the parallel polarized wave incidence up to 50° using CST Microwave Studio. However, Fig. 5b shows not any significant shift in the resonance frequency when the simulation is performed using Ansoft HFSS. In addition to this, Figs. 4 and 5 demonstrate that the proposed bandpass FSS structure provide wide-band characteristics in Ku-band.

For 25 GHz intended frequency, the value of *C* and *L* is 0.53 fF and 0.768 nH, respectively, which provides the resonance frequency 24.98 GHz for the normal wave incidence. Table 4 discusses the effect of the perpendicular and parallel polarized wave

**Table 4** Angular stability and 3-dB reflection/transmission bandwidth of the proposed bandpass FSS structure through CST Microwave Studio and Ansoft HFSS in Ka-band for perpendicular and parallel polarized wave

AOI	Parallel polarization											
	Perpendicular polarization						Parallel polarization					
	CST microwave studio			Ansoft HFSS			CST microwave studio			Ansoft HFSS		
$f_r$ (GHz)	3-dB BW (GHz)	FBW (%)	$f_r$ (GHz)	3-dB BW (GHz)	FBW (%)	$f_r$ (GHz)	3-dB BW (GHz)	FBW (%)	$f_r$ (GHz)	3-dB BW (GHz)	FBW (%)	
0°	25.042	2.113	8.4	25.2	2.2	8.7	25.070	2.037	8.1	25.2	2.1	8.3
10°	25.028	2.078	8.3	25.2	2.1	8.3	25.070	2.035	8.1	25.2	2.1	8.3
30°	25.028	2.072	8.2	25.2	2.1	8.3	25.056	2.029	8.0	25.2	2.1	8.3
50°	25.028	2.072	8.2	25.2	2.1	8.3	25.056	2.027	8.0	25.2	2.1	8.3

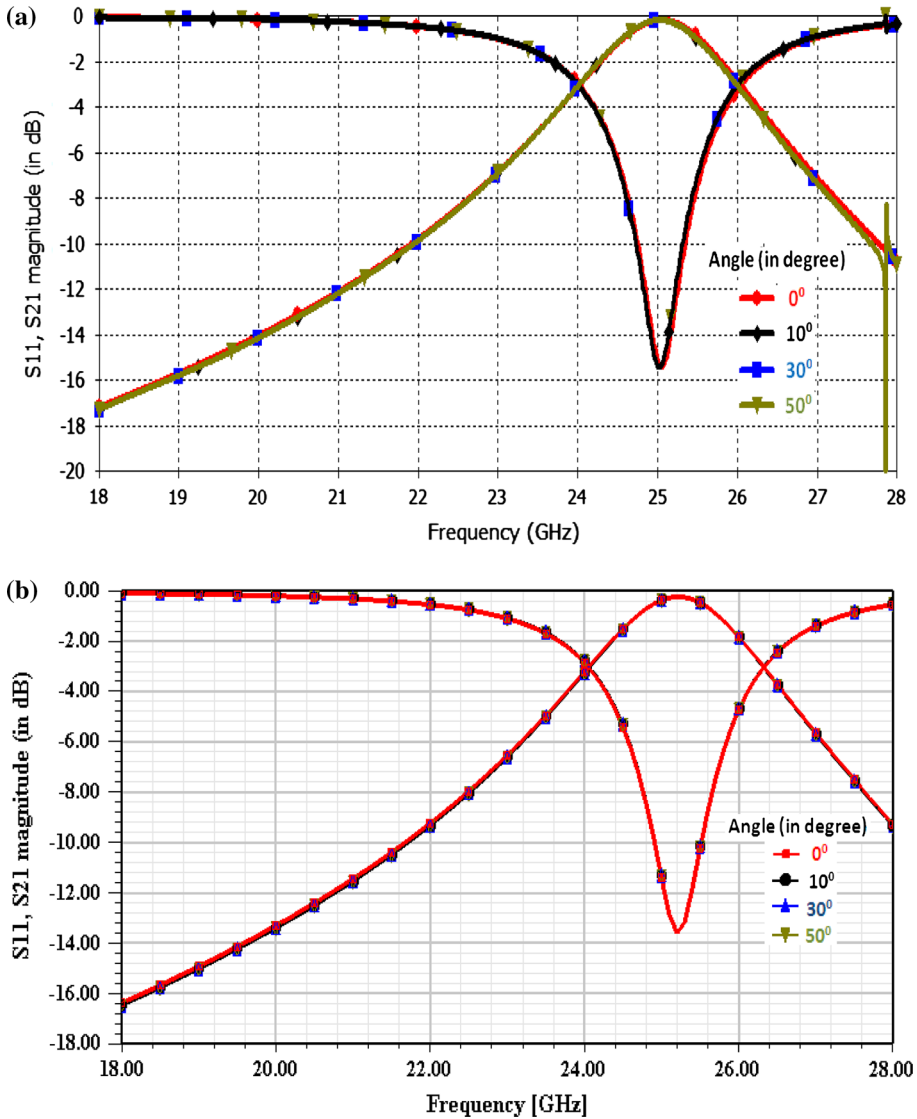


**Fig. 6** The frequency response of proposed bandpass FSS structure for perpendicular polarized wave at different AOI in Ka-band using (a) CST Microwave Studio and (b) Ansoft HFSS

incidence up to 50° AOI on the resonance frequency, 3-dB bandwidth and FBW of the proposed bandpass FSS structure. For the perpendicular polarized wave incidence up to 50° AOI, the resonance frequency of the proposed bandpass FSS structure downshift up to 0.055 % with reference to the normal incidence when the simulation has been performed by using CST Microwave Studio as shown in Fig. 6a. However, Fig. 6b shows no any significant shift in the resonance frequency when the simulation is performed using Ansoft HFSS. Figure 7a demonstrates 0.05 % downshift in the resonance frequency with reference to the normal wave incidence for the parallel polarized wave incidence up to 50°

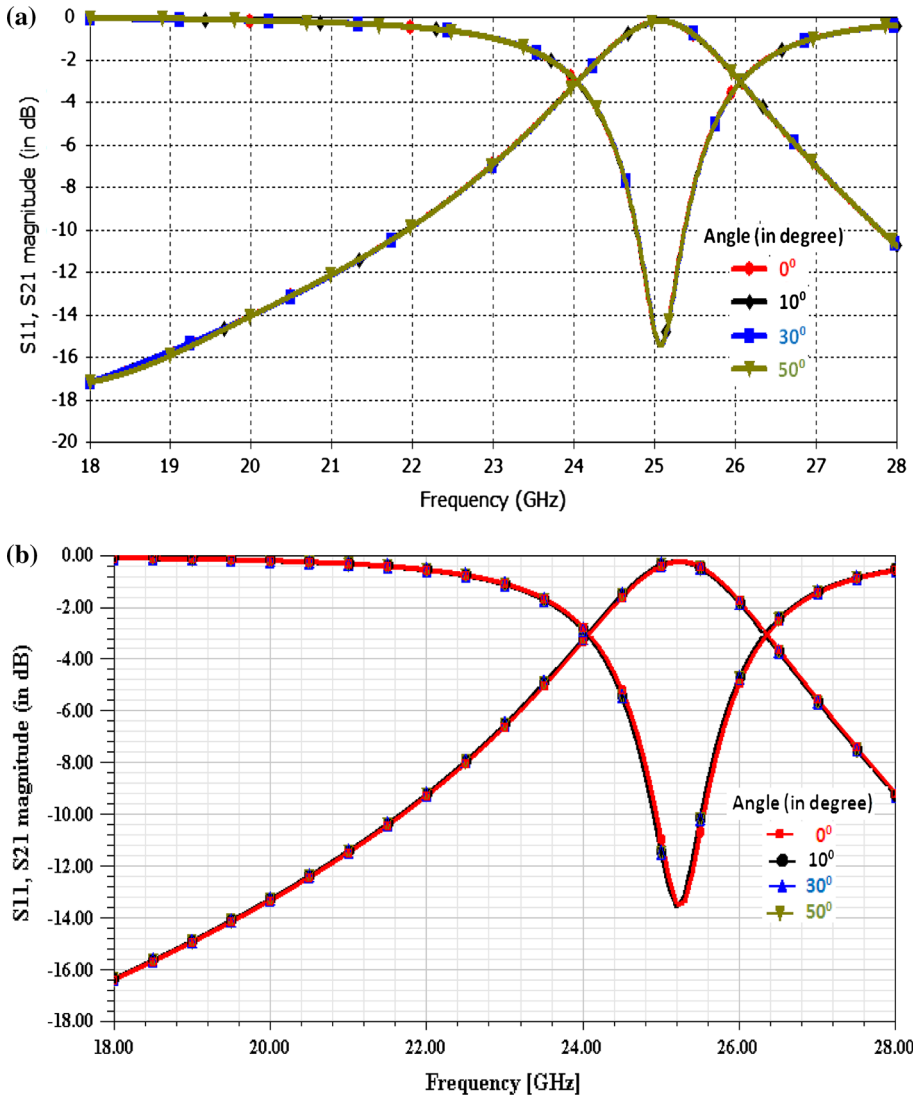


**Fig. 7** The frequency response of proposed bandpass FSS structure for parallel polarized wave at different AOI in Ka-band using (a) CST Microwave Studio and (b) Ansoft HFSS

using CST Microwave Studio. However, Fig. 7b shows no any significant shift in the resonance frequency when the simulation is performed using Ansoft HFSS. In addition to this, for the perpendicular and polarized wave incidence up to 50° AOI on the proposed bandpass FSS, the FBW of approximately 8.2 and 8 %, respectively is achieved, as presented in Table 4. Moreover, at each frequency of interest (i.e., 3, 15 and 25 GHz), the resonance frequency achieved theoretically, using CST Microwave Studio and Ansoft HFSS experiences a little deviation, which is due to the following reasons. (1) Use of different numerical techniques [i.e., equivalent circuit technique/transmission-line method is used to theoretically compute the resonance frequency (simpler and computationally in-

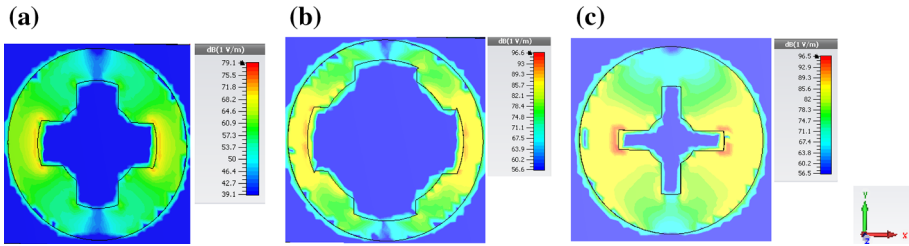


**Fig. 8** The electric field distribution of the proposed bandpass FSS structure at **a** 3.360, **b** 15.174 and **c** 25.2 GHz

**Table 5** Comparison of angular/polarization stability of the proposed bandpass FSS structure with other reported FSS literatures

AOI (in degree)	FSS structure	% Deviation of $f_r$
45	FSS structure in [22]	7 (TE and TM incidence)
45	FSS structure in [23]	16.6
45	FSS structure in [24]	7.60
45	FSS structure in [25]	5.45
45	FSS structure in [26]	5.00
45	FSS structure in [27]	5.95
45	FSS structure in [29]	3 (TE incidence) and 10 (TM incidence)
60	FSS structure in [30]	0.52 (TE incidence) and 2.1 (TM incidence)
60	FSS structure in [31]	~ 1 (TE and TM incidence)
60	FSS structure in [32]	~ 5 (TE and TM incidence)
60	FSS structure in [33]	~ 0.1 (TE incidence) and ~ 1.0 (TE-incidence)
50	Proposed FSS structure	0.65 (TE incidence) and 0.59 (TM incidence) (at 3 GHz) 0.013(TE incidence) and 0 (TM incidence) (at 15 GHz) 0 (TE incidence) and 0 (TM incidence) (at 25 GHz)

extensive), CST microwave Studio is based on finite integral technique [39] and Ansoft HFSS [40] is based on finite element technique], (2) The CST Microwave Studio and Ansoft HFSS take into account the effect of dielectric permittivity, loss tangent and metal conductivity to compute the resonance response, however, the theoretical computation of the resonance frequency (using equivalent circuit technique/transmission-line method) consider only the effect of dielectric permittivity but not the loss tangent and metal conductivity, and (3) Due to the different mesh types used in CST Microwave Studio and Ansoft HFSS.

### 3.2 Electric Field Distribution

The proposed bandpass FSS structure is designed at each frequency of interest (3, 15 and 25 GHz) using the geometrical parameters, which are shown in Table 1. The structure provides the resonance pole transmission at 3.360, 15.174 and 25.2 GHz for the normal wave incidence.

However, the electric field distribution diagram has the potential to justify the physical mechanism of the bandpass/bandstop filtering characteristics of the FSS structure [41], therefore, we have simulated the electric field distribution at 3.360, 15.174 and 25.2 GHz for the normal wave incidence. With the electric field distribution, we have observed that the electric field resonance occur in the aperture (proposed FSS structure) at 3.360, 15.174 and 25.2 GHz as shown in Fig. 8a, b and c, respectively. Moreover, the passband arises due to the enhanced transmission assisted by aperture resonance and outside the circular aperture, the electric field values are significantly weak.

Moreover, the comparison of angular and polarization stability of the proposed bandpass FSS with the other reported FSS structures are listed in Table 5, which demonstrates that the proposed structure provides significantly better angular and polarization stability up to  $50^\circ$  of AOI.

## 4 Conclusion

In this paper, an azimuthally periodic wedge-shaped circular ring bandpass FSS structure, which provides the angular/polarization stable frequency response with significant FBW in S-band, Ka-band and Ku-band, is discussed. The transmission-line method is used to obtain the lumped circuit elements of the proposed bandpass FSS structure, which offers less computation complexity as compared to that of the other numerical techniques. The proposed bandpass FSS structure provides approximately 59 % FBW in S-band and wide-band frequency characteristics in Ku-band, which is useful for the satellite communication. In addition to this, the proposed bandpass FSS is a single layer and low profile structure, which is very economic from practical perspectives.

**Acknowledgments** The authors are sincerely thankful to the anonymous reviewer for critical comments and suggestions to improve the quality of the manuscript and also to the Indian Space Research Organization vide Project No. ISRO/RES/4/579/10-11 for the financial aid.

## References

1. Munk, B. A. (2000). *Frequency selective surface: Theory and design* (1st ed.). New York: Wiley.
2. Zhang, L., Yang, G., Wu, Q., & Hua, J. (2012). A novel active frequency selective surface with wideband tuning range for EMC purpose. *IEEE Transactions on Magnetics*, 48(11), 4534–4537.
3. Te-Kao, W. (1994). Four-band frequency selective surface with double-square-loop patch elements. *IEEE Transactions on Antennas and Propagation*, 42(12), 1659–1663.
4. Bharti, G., Jha, K. R., Singh, G., & Jyoti, R. (2015). Design of angular and polarization stable modified circular ring frequency selective surface for satellite communication. *International Journal of Microwave and Microwave Technologies*. doi: [10.1017/S1759078715000331](https://doi.org/10.1017/S1759078715000331).
5. Gustafsson, M., Karlsson, A., Rebelo, A. P., & Widenberg, B. (2006). Design of frequency selective windows for improved indoor outdoor communication. *IEEE Transactions on Antennas and Propagation*, 54(6), 1897–1900.
6. Mias, C. Tsokonas, C. & Oswald, C. (2002). An investigation into the feasibility of designing frequency selective windows employing periodic structures. Technical report AY3922, The Nottingham Trent University, Burton Street, Nottingham, NG1 4BU, U.K.
7. Costa, F., Amabile, C., Monorchio, A., & Prati, E. (2011). Waveguide dielectric permittivity measurement technique based on resonant FSS filters. *IEEE Microwave and Wireless Components Letters*, 21(5), 273–275.
8. Genovesi, S., Costa, F., & Monorchio, A. (2012). Low-profile array with reduced radar cross section by using hybrid frequency selective surfaces. *IEEE Transactions on Antennas and Propagation*, 60(5), 2327–2335.

9. Raspopoulos, M., & Stavrou, S. (2011). Frequency selective buildings through frequency selective surfaces. *IEEE Transactions on Antennas and Propagation*, 59(8), 2998–3005.
10. Izquierdo, B. S., Parker, E. A., & Batchelor, J. C. (2011). Switchable frequency selective slot arrays. *IEEE Transactions on Antennas and Propagation*, 59(7), 2728–2731.
11. Li, B., & Shen, Z. (2014). Bandpass frequency selective structure with wideband spurious rejection. *IEEE Antennas and Wireless Propagation Letters*, 13, 145–148.
12. Bardi, I., Remski, R., Perry, D., & Cendes, Z. (2002). Plane wave scattering from frequency-selective surfaces by the finite-element method. *IEEE Transactions on Magnetics*, 38(2), 641–644.
13. Mittra, R., Chan, C. H., & Cwik, T. (1988). Techniques for analyzing frequency selective surfaces: A review. *Proceedings of the IEEE*, 76(12), 1593–1615.
14. Orta, R., Tascone, R., & Zich, R. (1985). A unified formulation for the analysis of general frequency selective surfaces. *Electromagnetics*, 5(4), 307–329.
15. Bozzi, M., & Perregrini, L. (1999). Efficient analysis of thin conducting screens perforated periodically with arbitrarily shaped apertures. *IEE Electronics Letters*, 35(13), 1085–1087.
16. Hsieh, L. H., & Chang, K. (2002). “Equivalent lumped elements G, L, C, and unloaded Q’s of closed- and open-loop ring resonators. *IEEE Transactions on Microwave Theory and Techniques*, 50(2), 453–460.
17. Langley, R. J., & Parker, E. A. (1983). Double-square frequency-selective surfaces and their equivalent circuit. *IEE Electronics Letters*, 19(17), 675–677.
18. Jha, K. R., Singh, G., & Jyoti, R. (2012). A simple synthesis technique of single square loop frequency selective surface. *Progress in Electromagnetic Research B*, 45, 165–185.
19. Costa, F., Monorchio, A., & Manara, G. (2012). Efficient analysis of frequency selective surfaces by a simple equivalent-circuit model. *IEEE Antennas and Propagation Magazine*, 54(4), 35–48.
20. Yao, X., Bai, M., & Miao, J. (2011). Equivalent circuit method for analyzing frequency selective surface with ring patch in oblique angles of incidence. *IEEE Antennas and Wireless Propagation Letters*, 10, 820–823.
21. Nair, R. U., & Jha, R. M. (2014). Electromagnetic design and performance analysis of airborne radomes: Trends and perspectives [Antenna Applications Corner]. *IEEE Antennas and Propagation Magazine, IEEE*, 56(4), 276–298.
22. Lee, C. K., & Langley, R. J. (1985). Equivalent-circuit models for frequency selective surfaces at oblique angles of incidence. *IEE Proceedings H on Microwaves Antennas and Propagation*, 132(6), 395–399.
23. Reed, J. A. (1997). Frequency selective surfaces with multiple periodic elements. Ph.D. thesis, The University of Texas, Dallas, 1997.
24. Sung, G. H. H., Sowerby, K. W., & Williamson, A. G. (2005). Equivalent circuit modelling of a frequency selective plasterboard wall. In *Proceedings of IEEE international symposium on antennas and propagation, Washington DC, USA, July 3–8* (pp. 400–403).
25. Hosseinpanah, M., Wu, Q., Zhang, C., Minji, F. A., & Yang, G. Y. (2008). Design of square-loop frequency selective surfaces utilize C-band radar stations. In *Proc. int. conf. on microwave and millimeter wave technology, 2008, Nanjing, China, April 21–24* (pp. 66–68).
26. Sung, H. H. (2006). Frequency selective wallpaper for mitigating indoor wireless interference. Ph.D. thesis, Auckland University, NZ.
27. Parker, E. A., & Hamdy, S. M. A. (1981). Rings as elements for frequency selective surfaces. *IEE Electronics Letters*, 17(17), 612–614.
28. Huang, J., Wu, T. K., & Lee, S. W. (1994). Tri-band frequency selective surface with circular ring elements. *IEEE Transactions on Antennas and Propagation*, 42(2), 166–175.
29. Izquierdo, B. S., & Parker, E. A. (2014). Dual polarized reconfigurable frequency selective surfaces. *IEEE Transactions on Antennas and Propagation*, 62(2), 764–771.
30. Yang, G., Zhang, T., Li, W., & Wu, Q. (2010). A novel stable miniaturized frequency selective surface. *IEEE Antennas and Wireless Propagation Letters*, 9, 1018–1021.
31. Chiu, C. N., & Wang, W. (2013). A dual-frequency miniaturized-element FSS with closely located resonances. *IEEE Antennas and Wireless Propagation Letters*, 12, 163–165.
32. Yan, M., Que, S., Wang, J., Zhang, J., Zhang, A., Xia, S., & Wang, W. (2014). A novel miniaturized frequency selective surface with stable resonance. *IEEE Antennas and Wireless Propagation Letters*, 13, 639–641.
33. Guang-Ming, T., Jun-Gang, M., & Jin-Ming, D. (2012). A novel four-legged loaded element thick-screen frequency selective surface with a stable performance. *Chinese Physics B*, 21(12), 1–8.
34. Bharti, Garima, Jha, K. R., Singh, G., & Jyoti, R. (2015). Azimuthally periodic wedge-shaped metallic vane loaded circular ring frequency selective surface. *International Journal of Microwave and Wireless Technologies*, 7(1), 95–106.

35. Dubrovka, R., Vazquez, J., Parini, C., & Moore, D. (2006). Equivalent circuit method for analysis and synthesis of frequency selective surfaces. *IEE Proceedings Microwaves, Antennas and Propagation*, 153(3), 213–220.
36. Langley, R. J., & Parker, E. A. (1982). Equivalent circuit model for arrays of square loops. *IEE Electronics Letters*, 18(7), 294–296.
37. Chang, K. (1996). *Microwave ring circuits and antennas*. New York: Wiley.
38. Bahl, I. (2003). *Lumped elements for rf and microwave circuits* (1st ed.). London: Artech House.
39. Planar EM Technical notes, CST Microwave Studio: Floquet Port help. <http://www.slideshare.net/bundahamka/cst-training-core-module-antenna-2>.
40. Planar EM Technical notes, Getting started with HFSS: Floquet Port help. <http://www.scribd.com/doc/27207025/Getting-Started-With-HFSS#scribd>.
41. Yang, Y., Wang, X. H., & Zhou, H. (2012). Dual-band frequency selective surface with miniaturized element in low frequencies. *Progress in Electromagnetic Research Letter*, 33, 167–175.



**Garima Bharti** passed her B. Tech. in Electronics and Communication Engineering, from Institute of Engineering and Emerging Technologies (IEET), Baddi, Himachal Pradesh University, India and M. Tech. in Electronics and Communication Engineering from Jaypee University of Information Technology, Solan, Himachal Pradesh, India in 2010 and 2012, respectively. Currently, she is pursuing her Ph.D. degree from the Jaypee University of Information Technology, Solan, Himachal Pradesh, She is also working as Project Assistant in ISRO funded project since July 2012. Her area of interest is RF and Microwave Communication.



**Kumud Ranjan Jha** passed the Under-Graduation and Post-Graduation Examinations in the Electronics and Communication Engineering branch in 1999 and 2007, respectively. Since 2007, he is an Assistant Professor in Shri Mata Vaishno Devi University, Katra, Jammu and Kashmir, India, and before joining this University, he has served in the Indian Air Force. In 2012, he was awarded with the Ph.D. Degree from Jaypee University of Information Technology, Solan, Himachal Pradesh, India and subsequently, in the same year while working on the concept of the gain and directivity enhancement of the Planar Terahertz Antennas, he was awarded with the Raman Fellowship for 1 year for the Post-Doctoral Study in United States of America from the University Grant Commission, Government of India, New Delhi, India. He is also a visiting professor to San Diego State University, California, USA. He has published a number of peer reviewed, research articles in the International Journals and Conferences. His area of research is Microwave/RF passive component design and Terahertz Electronics for the future wireless communication.



**Ghanshyam Singh** received Ph.D. degree in Electronics Engineering from the Indian Institute of Technology, Banaras Hindu University, Varanasi, India, in 2000. He was associated with Central Electronics Engineering Research Institute, Pilani, and Institute for Plasma Research, Gandhinagar, India, respectively, where he was Research Scientist. He had also worked as an Assistant Professor at Electronics and Communication Engineering Department, Nirma University of Science and Technology, Ahmedabad, India. He was a Visiting Researcher at the Seoul National University, Seoul, South Korea. At present, he is Professor with the Department of Electronics and Communication Engineering, Jaypee University of Information Technology, Wakanaghat, Solan, India. He is an author/co-author of more than 180 scientific papers of the refereed Journal and International Conferences. His research and teaching interests include RF/Microwave Engineering, Millimeter/THz Wave Antennas and its Applications in Communication and Imaging, Next Generation Com-

munication Systems (OFDM and Cognitive Radio), and Nanophotonics. He has more than 15 years of teaching and research experience in the area of Electromagnetic/Microwave Engineering, Wireless Communication and Nanophotonics. He has supervised various Ph.D. and M. Tech. theses. He has worked as a reviewer for several reputed Journals and Conferences. He is author of two books “Terahertz Planar Antennas for Next Generation Communication” and “MOSFET Technologies for Double-Pole Four-Throw Radio-Frequency Switch” published by Springer.



**Rajeev Jyoti** (SM'06) received the M.S. degree in physics and the M. Tech. degree in microwave electronics from Delhi University, Delhi, India, in 1984 and 1986, respectively. Since 1987, he has been involved in the development of antennas for satellite communication at the Space Applications Centre (SAC), Indian Space Research Organization (ISRO), Ahmedabad, India. Presently, he is Group Director of the Antenna Systems Group at SAC, ISRO, India. He has more than 25 years of experience in the development of space borne and ground antennas at SAC. He has contributed significantly to the design, analysis, and development of microwave antennas, namely gridded antennas, multiple beam antennas, and phased array antennas for INSAT/GSAT, RISAT, and DMSAR projects. He has published more than 55 papers in various conferences and referred journals and he holds 14 patents. Mr. Jyoti is a Fellow Member of IETE India and Chair of the Joint Chapter of IEEE AP and MTT, Ahmedabad. He was awarded the UN ESA Long Term Fellowship in Antenna and Propagation at ESTEC/ESA Noordwijk, The Netherlands.